Full length article

Fundamental insight into the effect of carbodiimide crosslinking on cellular recognition of collagen-based scaffolds

Daniel V. Bax [a,b,*], Natalia Davidenko [a], Donald Gullberg [c], Samir W. Hamaia [b], Richard W. Farndale [b,1], Serena M. Best [a,1], Ruth E. Cameron [a,1]

[a] Department of Materials Science and Metallurgy, University of Cambridge, 27 Charles Babbage Road, Cambridge CB3 0FS, United Kingdom
[b] Department of Biochemistry, University of Cambridge, Downing Site, Cambridge CB2 1QW, United Kingdom
[c] Department of Biomedicine, University of Bergen, Jonas Lies vei 91, Norway

ARTICLE INFO

ABSTRACT

Research on the development of collagen constructs is extremely important in the field of tissue engineering. Collagen scaffolds for numerous tissue engineering applications are frequently crosslinked with 1-ethyl-3-(3-dimethylaminopropyl-carbodiimide hydrochloride (EDC) in the presence of N-hydroxysuccinimide (NHS). Despite producing scaffolds with good biocompatibility and low cellular toxicity the influence of EDC/NHS crosslinking on the cell interactive properties of collagen has been overlooked. Here we have extensively studied the interaction of model cell lines with collagen I-based materials after crosslinking with different ratios of EDC in relation to the number of carboxylic acid residues on collagen. Divalent cation-dependent cell adhesion, via integrins $\alpha_1\beta_1$, $\alpha_2\beta_1$, $\alpha_{10}\beta_1$ and $\alpha_{11}\beta_1$, were sensitive to EDC crosslinking. With increasing EDC concentration, this was replaced with cation-independent adhesion. These results were replicated using purified recombinant I domains derived from integrin α_1 and α_2 subunits. Integrin $\alpha_2\beta_1$-mediated cell spreading, apoptosis and proliferation were all heavily influenced by EDC crosslinking of collagen. Data from this rigorous study provides an exciting new insight that EDC/NHS crosslinking is utilising the same carboxylic side chain chemistry that is vital for native-like integrin-mediated cell interactions. Due to the ubiquitous usage of EDC/NHS crosslinked collagen for biomaterials fabrication this data is essential to have a full understanding in order to ensure optimized collagen-based material performance.

Statement of Significance

Carbodiimide stabilised collagen is employed extensively for the fabrication of biologically active materials. Despite this common usage, the effect of carbodiimide crosslinking on cell-collagen interactions is unclear. Here we have found that carbodiimide crosslinking of collagen inhibits native-like, whilst increasing non-native like, cellular interactions. We propose a mechanistic model in which carbodiimide modifies the carboxylic acid groups on collagen that are essential for cell binding. As such we feel that this research provides a crucial, long awaited, insight into the bioactivity of carbodiimide crosslinked collagen. Through the ubiquitous use of collagen as a cellular substrate we feel that this is fundamental to a wide range of research activity with high impact across a broad range of disciplines.

1. Introduction

The extracellular matrix (ECM) of tissues is composed of a complex network of proteins, glycoproteins and glycosaminoglycans that surround cells. Purified components of the ECM have been widely employed in the design of tissue engineering scaffolds where they provide a similar cell niche to the native tissue [1]. Fibrillar collagen I is the most abundant ECM protein component, fulfilling both structural and cell adhesive roles in a wide range of

* Corresponding author at: Department of Materials Science and Metallurgy, University of Cambridge, 27 Charles Babbage Road, Cambridge CB3 0FS, United Kingdom.

E-mail address: dvb24@cam.ac.uk (D.V. Bax).
[1] These authors contributed equally.

tissue types [2]. Collagen I is a triple-helical protein which possesses the vital physical properties of strength and stiffness required for generating complex 3D structures [3]. Alongside its physical attributes, collagen I contains a series of cellular recognition motifs that interact with a diverse lineage of cells [4]. Therefore collagen I can provide appropriate physical support for a tissue replacement whilst simultaneously directing cell attachment, proliferation and differentiation. In addition to these physical and biological roles, collagen I can be isolated to high purity and is relatively inexpensive. As such there has been an explosion of interest in this area in recent years as evidenced by both recent publications and efficacious use in clinical products.

Collagen I interacts with cells via a number of cell surface receptors including integrins and discoidin domain receptors (DDRs) [4]. Integrins are a class of cell surface receptors that bind to a wide range of ECM proteins where each integrin contains a single α and β subunit. To date at least 18 α- and 8 β-subunits have been identified that dimerise to form at least 24 different integrin heterodimers [5]. Collagen I binds to four of these integrin heterodimers, all of which contain the β_1 subunit. These are integrins $\alpha_1\beta_1$, $\alpha_2\beta_1$, $\alpha_{10}\beta_1$, and $\alpha_{11}\beta_1$ [6,7]. Cell binding studies to libraries of collagen derived triple-helical sequences have identified numerous integrin-binding motifs within collagen [8]. This lead to the delineation of a GxxʹGExʺ consensus binding sequence for cell surface integrins $\alpha_1\beta_1$ and $\alpha_2\beta_1$ [4]. Although x may be phenylalanine (F), leucine (L), arginine (R), or methionine (M), of these combinations, the sequence GFOGER has been demonstrated as a high affinity integrin-binding site [8,9]. Integrins bind to collagen I via an inserted A domain (I domain) contained within the α subunit of the integrin. The crystal structure of the integrin α_2 I domain when interacting with a triple-helical GFOGER motif has been resolved [10]. This shows that the carboxylate side chain on the glutamic acid (E) residues of GFOG*E*R is critical for coordination with a Mg^{2+} ion within the metal ion-dependent adhesion site (MIDAS) on the I domain. As such, integrin-collagen interactions are highly dependent upon the presence of the divalent cation Mg^{2+}, making EDTA (ethylenediaminetetra-acetic) chelation of Mg^{2+} a convenient indicator for native-like integrin-mediated cell interaction.

In vivo collagen fibres are stabilised by enzymatic modification that leads to crosslinking. For biomaterials fabrication, similar physical integrity is obtained by carbodiimide chemical crosslinking using 1-ethyl-3-(3-dimethylaminopropyl-carbodiimide hydrochloride (EDC) in the presence of N-hydroxy-succinimide (NHS) [11]. By systematically modifying the EDC/NHS crosslinking regimes the physical properties of scaffolds can be modulated. This allows discrete control over the mechanical strength and degradation kinetics of the resultant scaffold [12]. During carbodiimide-mediated crosslinking the carboxylate moiety on one amino acid side chain (Asp, Glu) reacts through a condensation reaction with a primary amine on an adjacent amino acid (Lys). Standard crosslinking conditions of 11.5 mg/mL EDC (equivalent to 5xEDC: 2xNHS: 1xCOO⁻ group on collagen; 60 mM EDC) are defined as 100% throughout this paper, representing a 5-fold molar excess of the crosslinker compared to the molarity of carboxylate-containing side chains on collagen. This results in a measurable, dramatic loss of primary amine, and by extension, the carboxylate side chain content of the collagen-based scaffold [11]. This is of particular importance as the carboxylate anion of glutamic acid is critical for collagen ligation with integrins $\alpha_1\beta_1$ and $\alpha_2\beta_1$ and so we hypothesise that carbodiimide treatment of collagen could influence integrin-collagen ligation.

EDC/NHS crosslinking is frequently used to stabilise three-dimensional (3D) biomaterials with well-defined pore geometry [13,14] and percolation diameters [15] for optimal cell infiltration [16]. For this study we have focused on 2-dimensional films as an approximation to the pore walls of these 3-dimensional scaffolds

to reduce the complexity associated with 3D systems. The influence of EDC/NHS crosslinking on the physical properties, such as morphology, dissolution and mechanics of collagen-based scaffolds is well understood [11]. Despite this there are key areas of understanding, such as cellular interactions, that appear to have been overlooked. We have recently shown that EDC/NHS crosslinking of collagen-based materials influences cation dependent platelet and HT1080 cell attachment [11]. Therefore, the goal of this study was to explore the mechanism for this carbodiimide modulation of cell adhesion and to determine its influence on the cellular response. To do this we have analysed the cellular response to fibrillar collagen I treated with incremental dilution of EDC. We defined conventional levels of 11.5 mg/mL EDC as 100% and increased EDC and NHS concentrations up to 5-fold of this or diluted the concentration of EDC and NHS down to 1% of this condition whilst maintaining a constant collagen mass. We have utilised a range of model cell lines, each of which express unique collagen binding integrins. These have enabled us to probe the availability of specific integrin binding sites as a function of carbodiimide crosslinking. Through this research we demonstrate for the first time a detailed mechanism for cell-interaction with collagen materials crosslinked with increasing EDC/NHS conditions. Carbodiimide crosslinking of collagen is widely employed for biomaterials fabrication. This work provides a comprehensive investigation of the fundamental science that underpins this technology, producing scaffolds with appropriate physical and biological activity.

2. Materials and methods

2.1. Materials

Unless stated otherwise all reagents were analytical grade and used as received from Sigma-Aldrich.

2.2. Film preparation and crosslinking

Collagen slurries were prepared by swelling a 0.5% (w/v) suspension of bovine Achilles tendon insoluble collagen in 50 mM acetic acid at 4 °C overnight then homogenising on ice for 20 min at 13500 rpm using an Ultra-Turrax VD125 (VWR International Ltd., UK) homogeniser. Air bubbles were removed from the suspension by centrifuging at 2500 rpm for 5 min (Hermle Z300, Labortechnik, Germany). Films of ~8 μm of thickness were cast by pipetting 100 μL of slurry/well into an Immulon-2HB 96-well plate (Thermo Scientific) and drying for 48 h in a laminar flow cabinet.

Films were chemically crosslinked using EDC/NHS at molar ratios of EDC/NHS/COO⁻(Col) = 5/2/1 in 75% (v/v) Ethanol. This was defined as standard (100%) crosslinking conditions. The crosslinking solution was varied from this standard 100% condition by dissolving the appropriate amount of EDC/NHS into 75% Ethanol or by diluting from the 100% solution with 75% Ethanol. Non-crosslinked (0% EDC/NHS) films were incubated in 75% Ethanol only. After incubation for 2 h at room temperature the films were washed extensively with deionised water and dried in a laminar flow cabinet.

2.3. Platelet adhesion analysis

Platelets were obtained from human platelet rich plasma provided by the National Health Service Blood and Transplants (NHSBT) authority in accordance with the Declaration of Helsinki. Platelets were prepared by centrifugation for 15 min, 240g, the pellet discarded and 1 μL of Prostaglandin E₁ (100 μg/mL in ethanol)

added per mL of platelet supernatant. The platelet suspension was centrifuged at 640g for 10 min and the cell pellet resuspended in Tyrodes buffer (140 mM NaCl, 5.6 mM Glucose, 2 mM $MgCl_2$, 0.4 mM NaH_2PO_4, 12 mM $NaHCO_3$, 2.7 mM KCl, 10 mM HEPES pH 7.4) to a density of 1×10^8/mL (3.1×107/cm^2 well surface). Before platelet incubation, non-specific adsorption to the film or well was blocked with 200 μL of 5% w/v bovine serum albumin (BSA) in phosphate buffered saline (PBS) for 60 min, and then washed three times with 200 μL of PBS. 100 μL of platelet suspension containing either 5 mM Mg^{2+} or 5 mM EDTA, was added to wells and allowed to attach at room temperature for 30 min. The wells were washed with Tyrodes (200 μL x3) and then 150 μL of lysis buffer containing PNP phosphatase substrate (81 mM TriSodium Citrate, 31 mM Citric Acid, 0.1% v/v Triton X-00, 1.85 mg/mL PNP substrate, pH 5.4) was added for 90 min at room temperature. 100 μL of 2 M NaOH was added and the absorbance read at 405 nm (A_{405}) using a Fluostar Optima plate reader (BMG Labtech). Platelet adhesion assays were performed in quadruplicate and values are reported as means ± standard deviation.

2.4. Cell culture

HT1080 cells derived from a human fibrosarcoma were obtained from the European Collection of Animal Cell Cultures, Porton Down, UK. Rugli cells, derived from a rat glioma, were a kind gift from Dr. J. Gavrilovic, University of East Anglia, UK. The parent C2C12 mouse myoblast cells and C2C12 cells stably transfected with integrin α_1, α_2, and α_{11} were produced as described in [17]. C2C12 cells stably transfected with integrin α_{10} were a kind gift from Dr. E. Lungren-Åkerland, Xintela AB, Lund, Sweden. HT1080, Rugli and C2C12 mouse myoblast cell lines were maintained in a humidified incubator with 5% CO_2 at 37 °C in Dulbecco's modified Eagle's medium (DMEM, Sigma-Aldrich) containing 10% (v/v) fetal bovine serum (Sigma-Aldrich) and 1% (v/v) streptomycin/penicillin (Sigma-Aldrich). Cells were prepared for cell adhesion, spreading or annexin V analysis by detaching from the cell culture flasks with 0.05% (w/v) trypsin/0.02% (w/v) EDTA (Sigma-Aldrich) and re-suspending in serum free DMEM.

2.5. Cell adhesion analysis

Collagen films were BSA-blocked as for platelet adhesion analysis. 100 μL of cells was added to each well at a density of 5×10^5 cells/mL (equivalent to 1.56×10^5 cells/cm^2 of well surface) in serum-free DMEM containing either 5 mM $MgCl_2$ or 5 mM EDTA. After incubation at 37 °C/5%CO_2 for 45 min loosely-bound cells were removed with 3×200 μL PBS washes. Bound cells were detected using the phosphatase substrate as for platelet adhesion. Where shown, cation-dependent cell attachment was derived by subtracting the cell-derived absorbance in the presence of EDTA from that in the presence of $MgCl_2$. Values are means of quadruplicate measurements ± standard deviation.

For cation-dependent cell attachment analysis cells were added to each well at a density of 5×10^5 cells/mL (equivalent to 1.56×10^5 cells/cm^2 of well surface) in PBS containing the appropriate concentration of $MgCl_2$ or $CaCl_2$ instead of DMEM.

2.6. Cell spreading analysis

Collagen films were BSA-blocked as for platelet adhesion analysis. 100 μL of cells was added to each well at a density of 2.5×10^5 cells/mL (equivalent to 7.8×10^4 cells/cm^2 of well surface) in serum free DMEM. After incubation for 60 min, the cells were fixed for 20 min at room temperature by the addition of formaldehyde to the cell medium to achieve a final concentration of 3.7% (w/v). The wells were then extensively washed with PBS,

the wells filled with PBS then a glass slide layered across the well plate. Cell images were taken on a LEICA DMI6000CS phase contrast microscope fitted with a LEICA DFC340FX camera at 20× magnification. Cell spreading was quantified by scoring a cell as spread if it was phase-dark with cellular projections and a flattened morphology. Cells were scored as non-spread if rounded and phase-bright with no cellular projections as detailed in [18]. The percentage cell spreading was calculated by dividing the number of spread cells by the total number of cells present. Values are means of triplicate or quadruplicate measurements ± standard deviation

2.7. Integrin I domain binding analysis

Recombinant glutathione S transferase (GST) collagen binding I domains from integrin α_1 subunits and integrin α_2 subunits were expressed in *E. coli* and purified as described in [19]. Prior to I domain binding non-specific attachment to the collagen films was blocked with 5% (w/v) bovine serum albumin (BSA) in binding buffer (50 mM TRIS, 140 mM NaCl, 1 mg/mL BSA, pH 7.4) for 1 h at room temperature. Following BSA blocking, the samples were washed with 3×200 μL of binding buffer then incubated in 5 μg/mL recombinant integrin α_1 or α_2 I domain in binding buffer containing either 5 mM $MgCl_2$ or 5 mM EDTA. After 1 h incubation at room temperature, the samples were washed in 3×200 μL of binding buffer containing 5 mM $MgCl_2$ or 5 mM EDTA respectively. The presence of the GST tagged recombinant I domain was detected by incubating with 100 μL of 1:10,000 diluted HRP-conjugated goat anti-GST antibody (Life Technologies) for 20 min at room temperature. The detection antibody was removed and the films were washed with 4×200 μL of binding buffer for 20 min for each wash. 100 μL of TMB substrate (Thermo Scientific) was added to each well and the reaction was stopped by the addition of 100 μL of 2.5 M H_2SO_4 to each well. A_{450} was measured using a Fluostar Optima plate reader (BMG Labtech). Where shown, cation-dependent I domain binding was derived by subtracting the absorbance in the presence of EDTA from that in the presence of $MgCl_2$. Values are means of triplicate or quadruplicate measurements ± standard deviation

2.8. Amine group content correlation with cation-dependent cell adhesion

We have previously reported the free primary amine group content of collagen-based scaffolds crosslinked with increasing ratios of EDC and NHS to COO^- groups [11]. The number of free amine groups were derived from Fig. 4 in [11] as detailed in Supplementary Table 1. These free amine values were plotted against Mg^{2+} dependent cell attachment. Mg^{2+} dependent attachment was derived by subtracting adhesion in the presence of EDTA from adhesion in the presence of Mg^{2+}. Linear regressions were fitted to this data in Excel.

2.9. Annexin V analysis

Collagen films were BSA blocked and cell seeded as for cell spreading analysis. After 2 h incubation, the translocation of phosphatidylserine to the cell surface was determined using a FITC-conjugated Annexin V detection kit (AbCam) using the manufacturer's specifications. Briefly, the cell media was removed, the cell layer washed 2×500 μL of PBS then incubated with FITC conjugated Annexin V for 5 min in the dark. The cells were washed with 3×500 μL PBS then fixed with 3.7% (w/v) formaldehyde for 20 min. The formaldehyde was removed and the cell layer washed extensively with PBS before mounting onto a glass slide in Vector Shield (Vector Laboratories) and viewing on an Olympus FV300

laser-scanning confocal microscope. Fluorescent images of Annexin V and brightfield images of the total cell coverage were taken at 40× magnification. The percentage of Annexin V-positive cells was derived by dividing the number of fluorescently labelled cells (from the fluorescent image) by the total number of cells present (from the brightfield image).

2.10. HT1080 growth and surface coverage

200 µl of HT1080 cells at a density of 5×10^3 cell/mL (equivalent to 3.1×10^3 cells/cm^2 of well surface) in 10% FCS (v/v) containing DMEM were added to the films for either 1, 2, 3 or 5 days in a humidified incubator at 37 °C/5%CO_2. The cells were fixed through the addition of 37% (w/v) formaldehyde to a final concentration 3.7% (w/v) directly to the cell media for 20 min. The samples were washed extensively with PBS then the number of cells per field of view counted using a LEICA DMI6000CS phase contrast microscope fitted with a LEICA DFC340FX camera at 20× magnification. The results show the mean cells count per field of view for triplicate measurements ± standard deviations. The cell-occupied surface area was calculated from micrographs of the cell growth after 5 days in culture using Image J.

2.11. Patterned EDC/NHS crosslinking of films

EDC/NHS crosslinking solution was restricted to defined regions of collagen films by gently securing polypropylene tubing against the collagen film using clamps (Fig. 11 A). 200% crosslinking solution was prepared as for film crosslinking and applied to the lumen of the tubing for 2 h at room temperature. The crosslinker was removed and the crosslinked region of the sample was washed extensively with water before removing the tubing and allowing the sample to air dry.

2.12. Rhodamine Phalloidin staining of cells on patterned films

Samples were BSA-blocked and cell seeded as for cell adhesion analysis. These were incubated for 2 h at 37 °C/5%CO_2 then the cells were fixed by addition of formaldehyde directly to the cell medium to a final concentration of 3.7% (w/v). After 20 min incubation, the fixed cells were washed 3xPBS then permeabilised in 0.5% (v/v) Triton X-100 in PBS for 4 min. The samples were washed 3xPBS, then the cellular actin was stained with 1:10,000 diluted Rhodamine-conjugated Phalloidin (Molecular Probes) for 45 min at room temperature. The scaffolds were washed 3× QH$_2$O, mounted onto a glass slide using Vector mount (Vector Laboratories) and visualized using an Olympus FV300 laser scanning confocal microscope.

2.13. Statistical analysis

Unless otherwise stated all error bars indicate standard deviations from the mean. Statistical significance was determined with a student t-test with unequal variance where $*$indicates $p \leqslant 0.05$, $**$ indicates $p \leqslant 0.01$, $***$ indicates $p \leqslant 0.001$ and $****$ indicates $p \leqslant 0.0001$. All statistical annotation indicates the statistical difference between the data point annotated and the 0% crosslinker values.

3. Results

Cellular analysis was used to test if EDC crosslinking could modify integrin-mediated cell attachment to collagen-based biomaterials. To address this hypothesis the attachment of model cell lines, each expressing a single, specific collagen-binding integrin were measured.
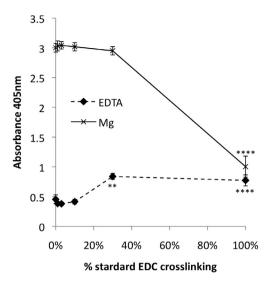
3.1. Platelet binding to EDC/NHS crosslinked collagen films

Platelets were chosen as an initial simple model system as they express a single collagen-binding integrin, $\alpha_2\beta_1$, for anchorage to collagen [20]. Integrin-mediated adhesion requires cations and so platelet binding was examined in the presence of the physiological cation, Mg^{2+} (metal-ion-mediated binding), or the cation chelator, EDTA (non-metal-ion-mediated binding). When added to collagen films crosslinked with increasing concentrations of EDC/NHS, the level of platelet adhesion was not perturbed with low doses of EDC/NHS (up to 30% of standard conditions), however increased levels of EDC/NHS crosslinking blocked platelet interactions in the presence of Mg^{2+} (Fig. 1). EDTA inclusion blocked platelet interactions with collagen films that had been crosslinked with up to 30% EDC/NHS. Therefore platelet binding to low dose EDC crosslinked collagen films is divalent cation-dependent. Interestingly, a small degree of platelet adhesion was observed in the presence of EDTA with EDC/NHS concentrations of 30% and above. As this adhesion occurred in the presence of EDTA this suggests that this adhesion is not mediated via the metal ion mediated binding site on integrin $\alpha_2\beta_1$. Moreover, by utilising lower than conventional (100%) crosslinking conditions the native platelet-collagen interactions can be preserved.

3.2. Integrin $\alpha_2\beta_1$ mediated HT1080 interactions with EDC crosslinked collagen films

HT1080 human fibrosarcoma cells predominantly utilise integrin $\alpha_2\beta_1$ for collagen binding, and have been widely used as a consequence [21,22]. Therefore these were chosen as a model cell line to examine the interaction of EDC/NHS crosslinked films with cellular-, rather than platelet-associated integrin $\alpha_2\beta_1$. Consistent with the platelet binding results, HT1080 cell ligation with collagen films was reduced by EDC/NHS crosslinking (Fig. 2A). HT1080 cell attachment in the presence of Mg^{2+} showed dose-dependent inhibition with up to 30% of standard EDC crosslinking conditions. Although 100% EDC crosslinking inhibited HT1080 cell attachment, this had not reached saturation and so it was not clear if this represented the maximal inhibition potential of EDC crosslinking. Therefore crosslinking was extended to 500% conditions resulting in a small decrease in HT1080 cell attachment over 100% conditions. Alongside the loss of HT1080 cell binding in the presence of Mg^{2+}, there was an increase in cation-independent binding, i.e. in the presence of EDTA, with increasing EDC/NHS crosslinking. This was particularly evident with EDC/NHS conditions of 30% and above, where cation-independent HT1080 binding in the presence of EDTA accounted for the majority of cell binding to the collagen films. Therefore, not only does conventional 100% chemical crosslinking of collagen films lower the overall level of HT1080 cell attachment, this crosslinking regime changes the mode of interaction from cation-dependent to cation-independent.

Cell spreading analysis was used to further explore the ability of EDC/NHS crosslinked films to elicit a cell morphology that reflects an intimate, physiological interaction with the substrate. HT1080 cell spreading displayed dose-dependent inhibition with increasing EDC/NHS crosslinking of the underlying collagen films (Fig. 2B). Little inhibition of HT1080 cell spreading was observed with crosslinking conditions up to 30% of the conventional EDC/NHS concentration. By contrast HT1080 cell spreading was inhibited with EDC/NHS concentrations above 30% with complete inhibition of cell spreading using a 200% crosslinking regime. It should be noted that cell spreading was conducted in the presence of Mg^{2+} as no cell spreading was observed for all crosslinking regimes in

Fig. 1. Effect of treating insoluble collagen films with increasing concentrations of EDC/NHS crosslinker on platelet adhesion (integrin $\alpha_2\beta_1$-dependent). 100% indicates a ratio of 5EDC:2NHS:1COO- group on collagen. The lower% EDC conditions represent dilution of EDC and NHS against COO- groups on collagen. Platelet adhesion was performed in the presence of 5 mM Mg^{2+} (cross, solid line) or 5 mM EDTA (diamond, dashed line). ** and **** indicate $p \leqslant 0.01$ and $p \leqslant 0.0001$ respectively in a student's t-test between the data point annotated and the 0% crosslinker values. Error bars indicate standard deviations from the mean.

the presence of EDTA [data not shown]. This pattern is reflected in the representative cell spreading micrographs in Fig. 2C. Using up to 30% EDC/NHS, the cells appear flattened with a phase dark appearance, however using high concentrations of crosslinker the cells are phase bright and rounded. Together, these data indicate that although HT1080 cells can attach to 100% EDC crosslinked collagen in a cation-independent manner this cannot support cell spreading.

EDTA acts to deplete the cell media (DMEM) of divalent cations, by chelating, for example, Ca^{2+} and Mg^{2+}, showing that divalent cation-dependent cell adhesion to collagen is influenced by EDC/NHS crosslinking. To extend this finding, cell assays were performed using PBS instead of DMEM as the cell media (Fig. 3A). PBS does not contain divalent cations and so this choice of cell media allowed for the selective inclusion of discrete and defined levels of divalent cations. Integrin mediated adhesion is stimulated by the presence of Mg^{2+} but not Ca^{2+} and so these were chosen for this analysis. HT1080 adhesion to non-crosslinked films was dependent upon the inclusion of 2 mM Mg^{2+}. Consistent with an integrin binding mechanism the inclusion of 2 mM Ca^{2+} did not stimulate HT1080 adhesion to non-crosslinked films. A similar pattern of cell adhesion was observed on collagen films crosslinked with up to 3% of conventional crosslinking conditions. After using 10% or 30% crosslinking, the degree of HT1080 adhesion in the presence of Mg^{2+} decreased. Conversely the degree of adhesion in the absence of cations or in the presence of Ca^{2+} increased. At 100% crosslinking, cell adhesion in the presence of Mg^{2+} increased up to levels observed on non-crosslinked samples, however the degree of adhesion in the absence of divalent ions or presence of Ca^{2+} increased compared with a 0% crosslinker control.

As the previous analysis was conducted in the presence of 2 mM cation, the dependence for cation co-ordination was further explored by including an increasing concentration of Mg^{2+} or Ca^{2+} (Fig. 3B). HT1080 cell adhesion to non-crosslinked collagen films was critically dependent upon the presence of Mg^{2+} whilst little adhesion was observed in the absence of cations. This increased dose-dependently with increasing Mg^{2+} concentration up to a saturating concentration of 1 mM Mg^{2+}. Conversely Ca^{2+}

did not stimulate cell adhesion to non-crosslinked collagen films at concentrations up to 2 mM, which is consistent with an integrin-mediated interaction. HT1080 adhesion was observed on 200% crosslinked collagen films in the absence of divalent cation. Inclusion of either Mg^{2+} or Ca^{2+} did not influence HT1080 adhesion to 200% crosslinked collagen films. Therefore these data show that HT1080 cells can adhere to EDC/NHS-crosslinked collagen in a divalent cation-independent manner that is different to native collagen binding in the absence of EDC/NHS crosslinking.

3.3. Integrin $\alpha_1\beta_1$ mediated Rugli interactions with EDC crosslinked collagen films
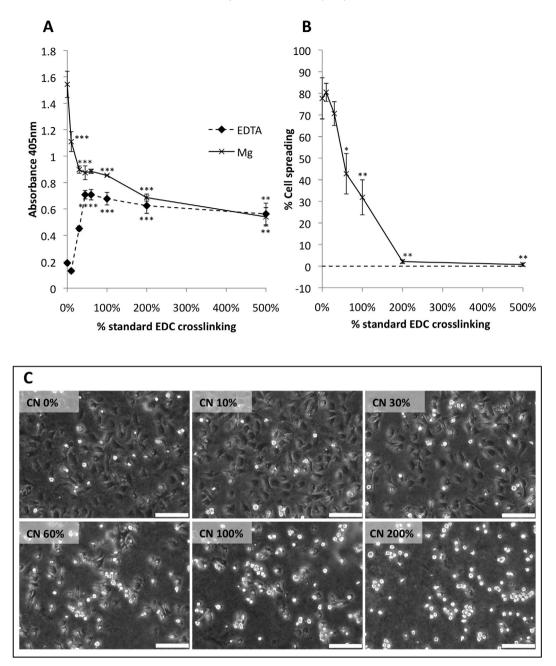
Rugli (rat glioma) cells bind to collagen predominantly through integrin $\alpha_1\beta_1$ [23]. Therefore Rugli cell attachment and spreading were measured to determine if EDC crosslinking modifies integrin $\alpha_1\beta_1$ binding to collagen-based materials. Integrin $\alpha_1\beta_1$-dependent Rugli attachment showed a biphasic response (Fig. 4A). In the initial phase, with increasing EDC crosslinking from 0% to 60% of standard EDC crosslinking conditions, there is a decrease in Mg^{2+}-dependent Rugli cell adhesion. Rugli adhesion to collagen crosslinked with up to 60% EDC crosslinking conditions was inhibited to background levels with EDTA. Interestingly, a second phase was noted with EDC conditions of 100% and above. More cell attachment was observed when using greater than 100% EDC crosslinking conditions. However this attachment was Mg^{2+}-independent. Therefore, Mg^{2+}-dependent integrin $\alpha_1\beta_1$-mediated cell attachment is inhibited by EDC crosslinking of collagen and is replaced with Mg^{2+}-independent attachment.

Analysis of integrin $\alpha_1\beta_1$-dependent Rugli cell spreading showed that Rugli cell spreading is highly sensitive to the degree of EDC crosslinking. EDC crosslinking conditions above 10% results in a rounded, phase bright cellular morphology (Fig. 4B,C). Therefore the loss of Mg^{2+}-dependent integrin $\alpha_1\beta_1$-mediated cell interaction, at high EDC/NHS concentrations, results in insufficient cellular cues to support cell spreading.

3.4. Purified integrin I domain binding to EDC/NHS cross-linked collagen films

Integrin $\alpha_1\beta_1$ and $\alpha_2\beta_1$ ligation with fibrillar collagen occurs through an inserted (I) domain. This is located in the α subunit of the integrin heterodimer. Recombinant constructs of the I domains of integrin α_1 and α_2, which can be expressed separately from the rest of the α subunit, purified and accurately folded for use in adhesion assays, were used to test for direct integrin-collagen engagement in a cell-free system. ELISA-based detection of I domain binding (Fig. 5A) shows that integin α_1 I domain ligation is inhibited in a dose-dependent manner with increasing EDC crosslinking of the underlying collagen films. Integrin α_1 I domain binding to non-crosslinked collagen was inhibited with EDTA but with increasing EDC crosslinking some binding was evident in the presence of EDTA. Indeed with 500% EDC crosslinking conditions all integrin α_1 I domain binding was cation-independent. A 'no I domain' control gave low absorbance values, showing specificity for the presence of the I domain.

The binding of the integrin α_2 I domain shows a biphasic behaviour with increasing chemical crosslinking. An initial decrease in cation-dependent binding was noted followed by an increase in cation-independent binding (Fig. 5C). In the absence of EDC/NHS crosslinking, the integin α_2 I domain binds in a cation-dependent (EDTA inhibitable) manner. This binding is reduced by crosslinking with up to 10% conventional chemical crosslinking conditions. With increasing chemical crosslinking above 10%, the binding of the integrin α_2 I domain increases dose-dependently with

A

B

C

CN 0% CN 10% CN 30%

CN 60% CN 100% CN 200%

Fig. 2. Effect of treating insoluble collagen films with increasing concentrations of EDC/NHS crosslinker on HT1080 (integrin $\alpha_2\beta_1$-dependent) adhesion (A), % spreading (B), and spreading micrographs (C). 100% indicates a ratio of 5EDC:2NHS:1COO- group on collagen, with lower values shown in appropriate panels. Cell adhesion was performed in the presence of 5 mM Mg^{2+} (cross, solid line) or 5 mM EDTA (diamond, dashed line). Assays were conducted in DMEM without serum proteins. The scale bar represents 100 µm. *, **, *** and **** indicate $p \leqslant 0.05$, $p \leqslant 0.01$, $p \leqslant 0.001$ and $p \leqslant 0.0001$ respectively in a student's t-test between the data point annotated and the 0% crosslinker values. Error bars indicate standard deviations from the mean.

increasing EDC crosslinking. This increase in binding is completely cation-independent as it is observed in the presence of EDTA.
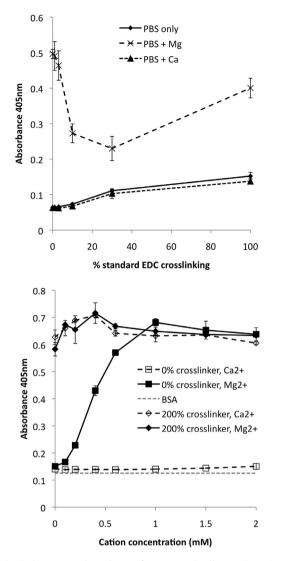
Interestingly, when cation-dependent binding is considered in isolation (Fig. 5B, D), both integrin α_1 and α_2 I domain binding is strongly inhibited by EDC crosslinking of the underlying collagen film.

3.5. Integrin α_2, α_{10}, and α_{11} transfected C2C12 cell interactions with EDC crosslinked collagen

C2C12 mouse myoblast cells do not endogenously express collagen-binding integrins, although they express the β_1 integrin subunit. Therefore specific integrin α subunits can be transfected

into these 'blank' cells. These transfected α subunits complex into collagen binding integrin α/β heterodimers through association with the cellular β_1 subunit. As such these cells are used to examine the binding characteristics of specific collagen binding integrins in isolation. To this end the binding of non-transfected C2C12 cells and C2C12 cells transfected with integrin α_2, α_{10}, and α_{11} were examined to establish the effect of EDC crosslinking on collagen ligation with these integrins (Fig. 6).

EDC crosslinking inhibited the Mg^{2+}-dependent attachment of C2C12 cells transfected with integrin, α_2, α_{10}, and α_{11} (Fig. 6B, C and D respectively). EDC crosslinking up to ~30% of standard conditions resulted in an approximately 50% reduction in cell attachment compared to non-crosslinked controls. No

Fig. 3. A) Divalent cation dependency of HT1080 cell adhesion (integrin $\alpha_2\beta_1$-dependent) to insoluble collagen I films treated with increasing concentrations of EDC/NHS crosslinker. 100% indicates a ratio of 5EDC:2NHS:1COO- group on collagen. Cell adhesion was conducted in PBS (diamond, solid line) or PBS supplemented with 2 mM Mg^{2+} (cross, long dashed line) or 2 mM Ca^{2+} (triangle, short dashed line). B) HT1080 cell adhesion to non-crosslinked (squares) or 200% crosslinked (diamonds) collagen I films when conducted in PBS supplemented with increasing concentrations of Mg^{2+} (solid symbol, solid line) or Ca^{2+} (open symbol, dashed line). A maximal cation concentration of 2 mM was used to prevent precipitation in PBS. Error bars indicate standard deviations from the mean.

Mg^{2+}-dependent attachment of non-transfected C2C12 cells (Fig. 6A) was observed. With EDC conditions above 30% an increase in Mg^{2+}-independent (in the presence of EDTA) attachment was observed for the non-transfected and all of the transfected C2C12 cells.

Spreading of integrin α_2- and α_{10}-transfected C2C12 cells was inhibited in dose-dependent manner with EDC crosslinking of the underlying collagen-based material (Fig. 7). EDC effectively reduced cell spreading to the non-transfected, 'blank' C2C12 cell spreading levels. Therefore the loss of the Mg^{2+}-dependent integrin α_2 and α_{10} mediated cell attachment by EDC treatment results in a lack of cell cues required for cell spreading. The Mg^{2+}-independent attachment observed with greater than 30% EDC crosslinking conditions is not capable of supporting cell spreading. Together these data show that EDC modifies integrin $\alpha_2\beta_1$-, $\alpha_{10}\beta_1$- and $\alpha_{11}\beta_1$-mediated cell engagement with collagen-based materials.

3.6. EDC crosslinking density and cell adhesion

Neighbouring carboxylate and amino groups are chemically modified during EDC crosslinking. Therefore the degree of chemical crosslinking was compared against the cell adhesion response (Fig. 8). Previously we have shown through TNBS detection that the number of free amine groups in the collagen films decreases with increasing EDC crosslinking [11]. Through the 1:1 chemical stoichiometry, this implies that the carboxylate groups are being similarly modified on the resulting material. Cation-dependent integrin-mediated attachment was used for this analysis as it depends critically upon carboxylate groups in the GxOGER and related motifs [4]. This was calculated by subtracting attachment in the presence of EDTA from cell adhesion in the presence of Mg^{2+}. From this analysis, there is a linear relationship between the number of free amine groups and the degree of cation-dependent attachment of HT1080 cells and α_2-, α_{10}-, and α_{11}-transfected C2C12 cells. The R^2 values ranged from 0.867 for α_{11}-transfected C2C12 cells to 0.998 for α_2-transfected C2C12 cells. Therefore there is a clear correlation between cation-dependent integrin mediated cell attachment and the extent of crosslinking of the collagen-based material.
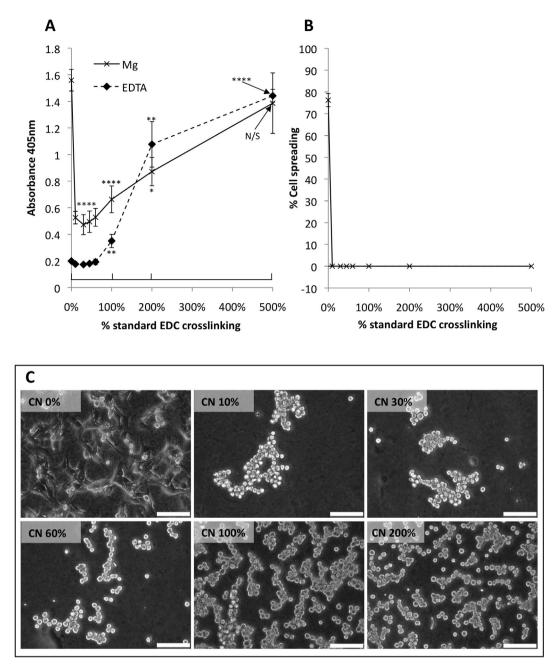
3.7. Cell viability and proliferation on EDC/NHS crosslinked collagen films

Phosphatidylserine translocation to the cell membrane, as measured by Annexin V staining, is a marker of programmed cell death. This was used to determine if the altered integrin-mediated cell binding to EDC/NHS crosslinked collagen films resulted in differential cell death. Fig. 9 A and B show that a small degree of Annexin V translocation was observed on 10% EDC/NHS crosslinked films, which increased with increasing EDC/NHS crosslinking up to 100% conditions. No further Annexin V translocation was observed with 200% EDC/NHS crosslinking. This shows that crosslinking conditions up to 10% EDC/NHS had little effect on HT1080 Annexin V translocation compared with 100% EDC/NHS crosslinking. Hence, EDC/NHS crosslinking is shown to alter the degree of cell death on the resultant films.

The degree of Annexin V translocation agreed with the ability of HT1080 cells to proliferate on EDC/NHS crosslinked collagen films (Fig. 10A). HT1080 cells proliferate from 19 ± 2.6 to 416 ± 20 cells per field of view over 5 days in culture on non-crosslinked controls. Crosslinking with 10% of standard conditions had no effect on the number of cells present compared with the non-crosslinked control. By contrast crosslinking conditions of 30% and above caused dose-dependent inhibition of cell growth. The lowest degree of cell growth was observed on 200% crosslinked collagen films where the number of cells per field of view increased from 15 ± 4 to 55 ± 30.4 over 5 days in culture. Similarly the degree of cell coverage after 5 days in culture was dependent upon the EDC/NHS crosslinking conditions (Fig. 10B). On non-crosslinked and 10% crosslinked collagen films approximately 99% of the surface was covered with cells. This cell coverage decreased with increasing EDC/NHS crosslinking to approximately 22% cell coverage with 200% EDC/NHS crosslinking conditions.

3.8. Cell adhesion to patterned EDC/NHS crosslinked collagen films

The previous results have compared separate, individual collagen films showing that they possess differing cell binding affinity depending upon the degree of EDC/NHS crosslinking. By restricting crosslinking to defined regions of the collagen film we have prepared patterned EDC/NHS crosslinked samples (Fig. 11A). Consistent with the previous data, HT1080 cells exclusively interacted with the non-crosslinked regions of the scaffold with minimal cells
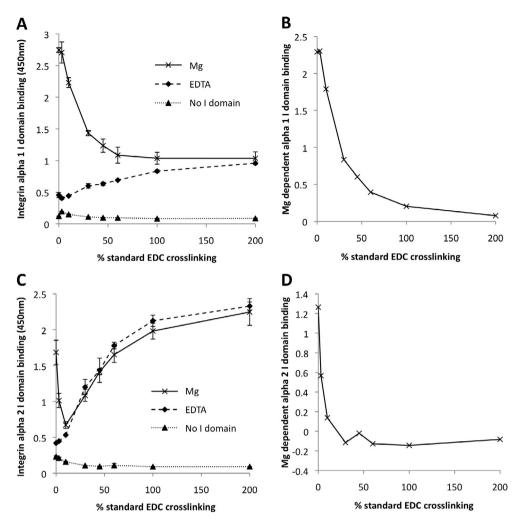
Fig. 4. Effect of treating insoluble collagen films with increasing concentrations of EDC/NHS crosslinker on Rugli (integrin $\alpha_1\beta_1$-dependent) adhesion (A),% spreading (B) and spreading micrographs (C). 100% indicates a ratio of 5EDC:2NHS:1COO- group on collagen. Cell adhesion was performed in the presence of 5 mM Mg^{2+} (cross, solid line) or 5 mM EDTA (diamond, dashed line). Assays were conducted in DMEM without serum proteins. The scale bar represents 100 μm. *, **, and **** indicate $p \leqslant 0.05$, $p \leqslant 0.01$, and $p \leqslant 0.0001$ respectively in a student's t-test between the data point annotated and the 0% crosslinker values. Error bars indicate standard deviations from the mean.

in the 200% crosslinked region (Fig. 11B). This patterning occurred within the length scale of a single cell where cells would conform sharply to the boundary between the crosslinked and non-crosslinked regions. Therefore the influence of EDC/NHS crosslinking can be observed simultaneously on a single sample. Moreover this technology allows, for the first time, for highly refined patterning of cellular distributions on a collagen-based scaffold by applying spatially confined EDC/NHS crosslinking.
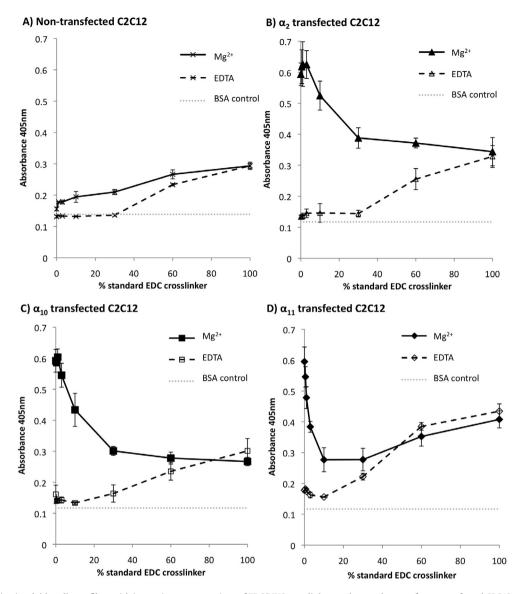
4. Discussion

To date there is no detailed mechanistic understanding of cell adhesion to carbodiimide-crosslinked collagen-based biomaterials.

Here we offer new insight into this important aspect of scaffold development that has been largely overlooked. Thin films were used as a model for the pore walls of a bulk scaffold as cells appear to interact predominantly with the wall material of porous 3-dimensional scaffolds. Although it is important to consider the bulk material properties, the use of 2D films enables us to reduce the complexity of the material to allow easy and uniform detection of cells, and so fully characterise the scaffold–cell interaction. Our research interest focused on universal platform technologies for biomaterials fabrication. Hence, we explored the presence of cell adhesion sites on collagen by using model cell lines and purified integrin I domains. This approach allowed us to provide a comprehensive understanding of the fundamental interactions between cells and carbodiimide-modified collagen.

Fig. 5. Binding of recombinant I domains derived from integrin α_1 (A,B) or α_2 (C,D) to insoluble collagen I films treated with increasing concentrations of EDC/NHS crosslinker. 100% indicates a ratio of 5EDC:2NHS:1COO- group on collagen. I domain binding was performed in the presence of 5 mM Mg^{2+} (cross, solid line) or 5 mM EDTA (diamond, long dashed line). A no-I domain control is shown (triangle, short dashed line). Mg^{2+}-dependent I domain binding was calculated by deducting the binding in the presence of EDTA from the adhesion observed in the presence of Mg^{2+} (B,D). Error bars indicate standard deviations from the mean.
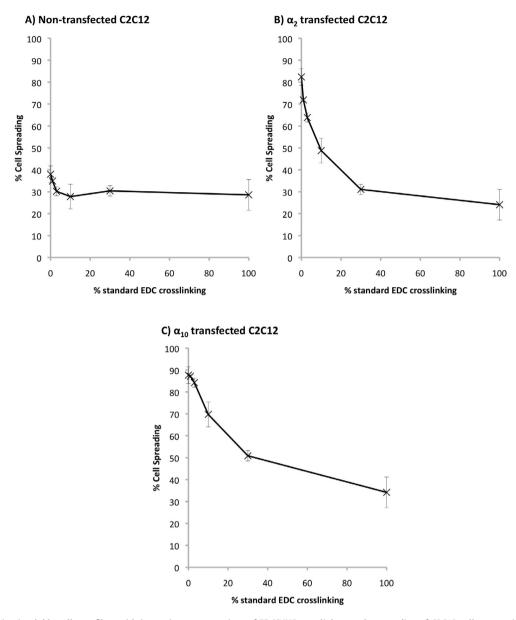
Using amine content analysis, we have previously shown that we can generate collagen-based materials with a range of crosslinking saturations [11]. This was achieved by altering the ratio of EDC/NHS crosslinker in respect to the number of carboxylic acid groups present on collagen. For this paper we have assigned the often used ratio of 5xEDC: 2xNHS: 1xCOO⁻ group on collagen as our standard (100%) crosslinking condition as this has been shown to produce scaffolds with appropriate degradation kinetics and optimal mechanical properties [11]. Through this approach of employing lower or higher ECD/NHS: COO⁻ ratios here we have shown that the carbodiimide crosslinking status also alters cellular engagement in a carbodiimide dose-dependent manner. Divalent cation-dependent integrin mediated adhesion of platelets, HT1080, Rugli and integrin α_2-, α_{10}-, and α_{11}-transfected C2C12 cells were all sensitive to carbodiimide treatment. Each cell line ligates collagen through one specific collagen binding integrin allowing us to deduce that collagen binding to all four collagen binding integrins, namely $\alpha_1\beta_1$, $\alpha_2\beta_1$, $\alpha_{10}\beta_1$ and $\alpha_{11}\beta_1$, is sensitive to carbodiimide crosslinking. Although conventional 100% crosslinking ablated native-like attachment, a lower EDC/NHS concentration of up to 10% of standard conditions could retain native-like integrin engagement. These studies are in agreement with a number of literature reports, however they conflict with others who have shown cytocompatibility of carbodiimide-crosslinked

collagen scaffolds. Indeed these conflicting results in the literature have prompted others to initiate a library of collagen-based materials in an attempt to establish the material parameters that are important for fibroblast and keratinocyte cell interactions [24]. Consistent with our data, the equivalent of 100% crosslinking conditions has been shown to reduce the number of integrin α_2 transfected C2C12 cells, HT1080 fibrosarcoma and rat glioma (Rugli) cells on collagen films [25–27]. Moreover increasing EDC/NHS crosslinking decreases the number of tendon cells present on collagen fibres [28,29]. Others have observed a similar effect for 3T3 pre-osteoblast proliferation on collagen-chondroitin 6 sulphate composites [30], for 3T3 fibroblasts on collagen-based nerve guides [31] and mouse fibroblasts interaction with collagen gels [32]. Meanwhile others have noted viability and proliferation of a wide variety of cell lineages on EDC-crosslinked collagen based and decellularised dermal materials [33–37].

It should also be noted that unlike our study, using increasing EDC/NHS crosslinking, many of these previous studies used a single molarity of EDC/NHS and often omit a non-crosslinked control. In this study we assigned a molar ratio of 5xEDC: 2xNHS: 1xCOO⁻ on collagen as our benchmark 100% crosslinking condition. In this instance we crosslinked a total mass of 0.5 mg collagen/film, equating to an EDC concentration of 11.5 mg/ml (60 mM) to satisfy the molar ratio of 5xEDC to 1xCOO⁻ group. This EDC concentration

Fig. 6. Effect of treating insoluble collagen films with increasing concentrations of EDC/NHS crosslinker on the attachment of non-transfected C2C12 cells (A) and C2C12 cells expressing integrin α_2 (B), α_{10} (C), and α_{11} (D). 100% indicates a ratio of 5EDC:2NHS:1COO- group on collagen. Cell adhesion was performed in the presence of 5 mM Mg²⁺ (solid line) or 5 mM EDTA (long dashed line). A negative BSA coated control is shown with a short dashed line. Assays were conducted in DMEM without serum proteins. Error bars indicate standard deviations from the mean.

is higher than some literature values however the ratio of EDC/NHS to collagen derived COO- groups is not stated in these publications. This makes direct comparison to our results difficult as we cannot calculate the EDC:COO⁻ molar ratio used in other studies. Furthermore differing cell analysis methods have been used for each study. For example many of the literature reports use prolonged cell cultures of between 3 and 14 days culture. Instead we have examined the cellular response over a series of time scales including adhesion (45 min), cell spreading (60 min), programmed cell death (2 h) and cell growth (1–5 days). The influence of culture time and the presence of serum are evidenced here. For example, although HT1080 cells did not spread at 60 min in the absence of serum on EDC crosslinked films, they proliferated on 100% crosslinked collagen in the presence of serum, albeit at a much slower rate than on non-crosslinked controls. Over time, cells will often remodel and secrete their own ECM and so the initial response to a biomaterial may become obscured during time in culture. Additionally, long-term assays require the presence of serum proteins in the cell media. Serum contains many proteins, such as fibronec-tin and vitronectin, which are potent cell adhesion molecules, binding different integrins than used here, [38,39] that also contain collagen-binding sites [40,41]. This dual collagen- and cell-binding activity means that within a serum-containing culture system it is not always clear that cells are responding to the native material chemistry or rather, whether adsorbed serum proteins are bridging between the scaffold and the cell. This influence of serum is evidenced from data published by Her et al. who observed increased human mesenchymal stem cell proliferation on low-dose crosslinked collagen-HA composites, but only in the presence of growth media [42]. Despite the possibility that serum proteins could facilitate cell binding to collagen based materials, in our hands we observed a decrease in proliferation with increased EDC/NHS crosslinking even in the presence of serum. To overcome the influence of serum proteins on the material–cell interaction we have undertaken our cell adhesion, spreading and apoptosis studies in serum-free conditions, allowing examination of direct cell–material interaction without influence from serum derived adhesive proteins. Although these cell assays were conducted in
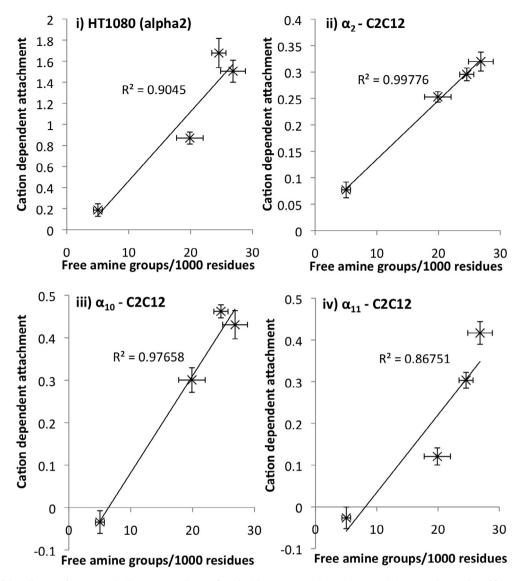
Fig. 7. Effect of treating insoluble collagen films with increasing concentrations of EDC/NHS crosslinker on the spreading of C2C12 cells expressing no collagen binding integrins (A) or expressing integrin α_2 (B) or α_{10} (C). 100% indicates a ratio of 5EDC:2NHS:1COO- group on collagen. Cell spreading was conducted in DMEM without serum proteins. Error bars indicate standard deviations from the mean.

serum-free conditions, a bovine serum albumin blocking step was included prior to cell incubation to prevent non-specific adhesion to the plastic well plate. Using this experimental approach, we have clearly shown that by increasing or decreasing the carbodiimide crosslinking concentration, the native-like cell adhesion to collagen can be ablated or retained respectively. Therefore our data suggest that the differing cellular responses cited in the previous studies may simply reflect the differing carbodiimide crosslinking conditions and cell analysis methodology employed.

To measure the degree of cell adhesion, we have adapted the well-accepted methodology detailed in [18]. This method was specifically chosen as it uses a moderate (3 wash) regime to remove loosely-bound cells from the material surface, making it suitable for measuring a wide range of cell-binding affinities. It is therefore possible that our choice of methodology has allowed us to identify novel non-metal ion-dependent cell binding with NHS/EDC crosslinked materials. Indeed using a more stringent washing regime [43] we have noted that the degree of non-metal

ion-dependent cell association is lower than reported here. This influence due to the stringency of the washing regime employed may imply that non-metal ion-dependent cell binding to EDC/NHS crosslinked materials is of lower affinity than native collagen binding. Cell-binding affinity modulates cellular function and so this may be responsible for the ablated cell spreading and proliferation on EDC/NHS crosslinked collagen.

Integrins $\alpha_1\beta_1$ and $\alpha_2\beta_1$ bind to collagen via inserted A domains (I domains) within the α-subunit [6]. Therefore, solid phase analysis of isolated integrin I domain binding to carbodiimide treated collagen was used to verify our cell-based data. Consistent with Rugli ($\alpha_1\beta_1$-dependent) and HT1080 ($\alpha_2\beta_1$-dependent) cell binding data, collagen association with isolated I domains from integrin α_1 and α_2 was sensitive to the degree of carbodiimide crosslinking. These solid-phase binding assays are cell-free, measuring direct collagen-integrin association, thereby corroborating that direct integrin $\alpha_1\beta_1$ and $\alpha_2\beta_1$ ligation with collagen is carbodiimide crosslinking-dependent. Additionally, the solid phase binding data
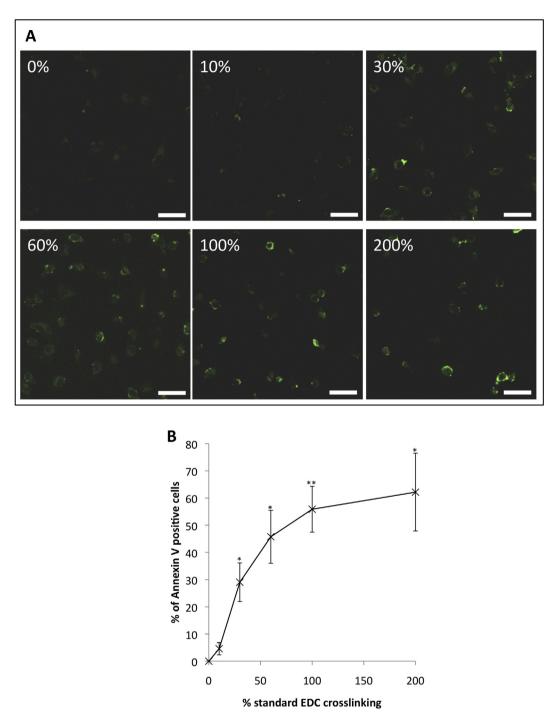
Fig. 8. Comparison of the adhesion of HT1080 cells (i) or C2C12 cells transfected with integrin α_2 (ii), α_{10} (iii) or α_{11} (iv) against the number of free amine groups present in the carbodiimide crosslinked film obtained from [11] and shown in Supplementary Table 1. Cation-dependent cell adhesion was calculated by deducting the binding in the presence of EDTA from that observed in the presence of Mg^{2+}. Error bars indicate standard deviations from the mean. The trend line represents linear regression fits to the data. The R^2 values indicate the fit between the data and the linear regression trend line.

also show that carbodiimide crosslinking reduces metal ion-dependent binding but increases metal ion-independent binding. A similar observation was evident from the cell binding data where all of the cell lines tested exhibited an increase in metal ion-independent binding in the presence of EDTA with increasing crosslinking. Interestingly this metal ion-independent attachment did not result in cell spreading or cell proliferation. Therefore, it appears that carbodiimide treatment inhibits native-like metal ion-dependent attachment and instead supports non-physiological metal ion-independent binding with subsequent effects on the cell phenotype. To further analyse this response we examined the metal ion dependency of attachment to carbodiimide crosslinked collagen. For this analysis cells were resuspended in cation-free buffer into which exogenous cations were applied. This controlled for any potential non-specific activity of the divalent cation chelator, EDTA, showing that cell adhesion to non-crosslinked collagen was dependent upon the presence of Mg^{2+}. By contrast cell adhesion to carbodiimide-crosslinked collagen was not sensitive to the presence of Mg^{2+}. Therefore, in addition to influencing the degree of cell adhesion, carbodiimide
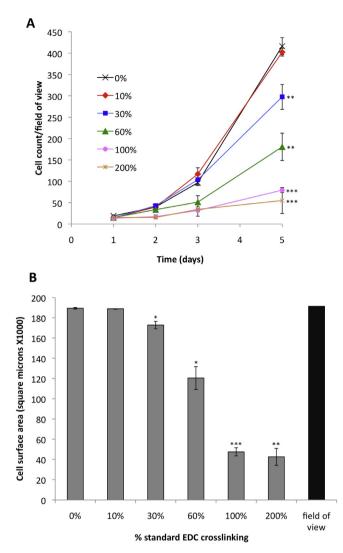
alters the mode of interaction. The reason for this increase in non-metal ion-dependent binding is not clear, however we postulate that this could be due to the EDC-derived peptide bonds which effectively alter the amino acid sequence and composition exposed on the surface of the collagen material. The intermediates of the EDC/NHS crosslinking reaction are unstable and so should not remain in the final scaffold. However at higher crosslinking conditions it is possible that the EDC reaction has not run to completion, thereby leaving potentially reactive groups on the scaffold that could bond to cells or purified I domains, resulting in non-specific binding in the presence of EDTA. Despite this possibility we feel that this is unlikely as we include a serum albumin passivating step prior to cell analysis. If incomplete EDC/NHS chemistry was present on the collagen scaffold then this should react with the serum albumin blocker and so are consumed before the addition of cells.

It is intriguing to hypothesise here the potential molecular mechanism behind these finding. Upon crosslinking, several properties of collagen films are altered, including decreased roughness, increased stiffness as well as loss of amine groups [25,26]. Through

Fig. 9. A) Influence of treating insoluble collagen films with increasing concentrations of EDC/NHS crosslinker on the translocation of phosphatidylserine across the plasma membrane in HT1080 cells as measured by fluorescent imaging of FITC conjugated Annexin V staining. Fluorescently labelled cells show phosphatidylserine translocation, a maker of apoptosis. B) Quantification of FITC-Annexin V staining from (A). The percentage of Annexin V positive (apoptotic) cells was calculated by dividing the number of fluorescently labelled cells by the total number of cells from a corresponding phase contrast image (not shown). 100% indicates a ratio of 5EDC:2NHS:1COO- group on collagen. Assays were conducted in DMEM without serum proteins. Scale bars indicate 100 μm. *, ** and *** indicate $p \leqslant 0.05$, $p \leqslant 0.01$ and $p \leqslant 0.001$ respectively in a student's t-test between the data point annotated and the 0% crosslinker values. Error bars indicate standard deviations from the mean.
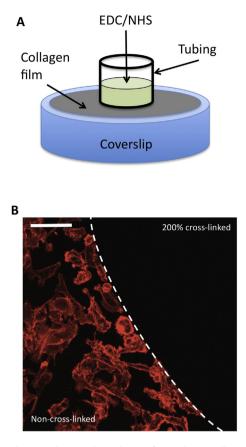
their adhesion receptors and cytoskeleton, cells can respond to a variety of cues including stiffness, roughness and chemistry. Therefore it is possible that the cell adhesion results observed could be attributed to one or indeed a combination of these parameters. On the other hand, within our isolated integrin I domain binding assays it would be difficult to rationalise why the surface stiffness and roughness would alter the I domain binding as there is no mechanotransductive apparatus associated with an isolated I

domain. Hence, it would appear that the material chemistry is the most probable reason for the altered integrin-binding properties of carbodiimide-crosslinked collagen. This is evidenced by the correlation between the number of free amines present on the collagen and divalent cation-dependent adhesion through integrins $\alpha_2\beta_1$, $\alpha_{10}\beta_1$ and $\alpha_{11}\beta_1$. Integrins bind to a series of motifs within collagen which often contain a Gxx′GEx″ consensus motif where x is a hydrophobic residue, x′ is usually hydroxyproline

A

B

Fig. 10. Effect of treating insoluble collagen films with increasing concentrations of EDC/NHS crosslinker on the growth (A) and cell surface coverage (B) of HT1080 cells over 5 days in culture. The cell number was counted manually and the cell area determined using Image J from phase contrast images. The cell surface coverage was determined after 5 days of culture. 100% indicates a ratio of 5EDC:2NHS:1COO-group on collagen. Cell proliferation was conducted in DMEM with the inclusion of 10% fetal bovine serum. A field of view bar (black) is shown in (B) to indicate the maximal potential area of cell surface coverage. *, ** and *** indicate p ⩽ 0.05, p ⩽ 0.01 and p ⩽ 0.001 respectively in a student's *t*-test between the data point annotated and the 0% crosslinker values. Error bars indicate standard deviations from the mean.

A

B

Fig. 11. A) Schematic showing the technique for producing collagen films with discrete areas of crosslinking. EDC/NHS crosslinking was restricted by adding EDC/NHS solution to the lumen of a polyethylene tube placed against the collagen film. B) Confocal fluorescence microscopy of rhodamine-phalloidin stained HT1080 cells adhering to collagen films crosslinked in defined locations with 200% crosslinker solution. The white dashed line indicates the boundary between the crosslinked and non-crosslinked regions of the film. The scale bar indicates 100 μm.

and x″ is often arginine [Reviewed in [4]]. Integrin binding to these motifs critically requires coordination between the carboxylate anion on the glutamic acid side of collagen and a Mg^{2+} ion held within the MIDAS of the integrin I domain (Fig. 12A). These same carboxylate moieties on collagen are crosslinked to proximal amine groups during EDC/NHS crosslinking. Consequently, it appears that EDC/NHS crosslinking and Mg^{2+}-dependent integrin binding require identical chemical groups. This offers a very likely explanation for our findings that excessive crosslinking inhibits integrin-dependent cell adhesion through chemical modification of critical carboxylic acid side chains on cell binding motifs (Fig. 12B).
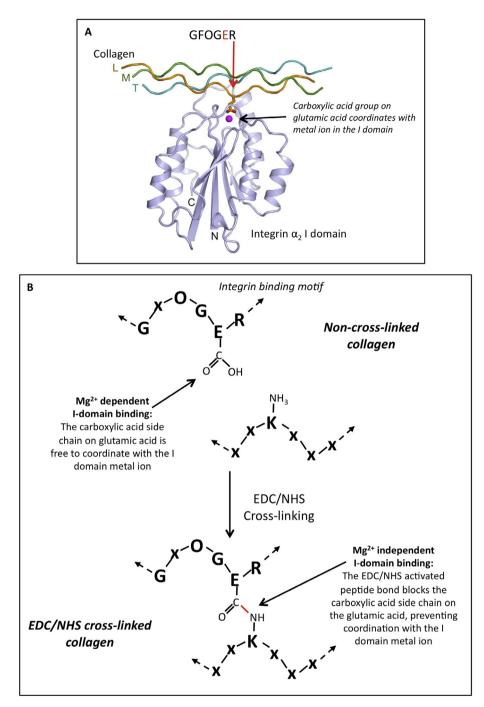
The ability to place cells discretely onto biomaterials is fundamental for numerous applications such as tissue engineering of complex structures, the fabrication of cell-based diagnostic chips, cell separation techniques and the detailed study of cellular biol-

ogy [44]. By crosslinking collagen films in pre-defined locations we have shown that we can position cells on a collagen-based biomaterial with high fidelity. Previous attempts to position cells have used techniques such as micro-contact printing, micro-lithography, PDMS micro-patterning or micro-fluidics [45–47]. These methods are often associated with high cost, complex methodology or do not utilise native cell binding proteins. By contrast the use of selective crosslinking of collagen, as shown here, is simple and does not require complicated fabrication processing. Moreover cell binding to the non-crosslinked regions is via native-like integrin-collagen interactions. As such our finding that EDC/NHS influences cellular attachment to collagen has allowed us to produce collagen based materials that support defined areas of cellular integration. Alongside producing patterned cellular distributions this data also show that the cellular response to differential crosslinking regimes can be measured simultaneously on a single sample. This effectively mitigates for any potential artefacts that could occur when measuring separate samples.

Currently, there is an unmet need for a biomaterial scaffold that can act as a cell support whilst also possessing tuneable mechanics and degradation kinetics for use in tissue engineering and replacement. In our previous studies we have shown that EDC/NHS crosslinking can be reduced to 10% of conventional conditions without affecting the stability and mechanics of the resultant scaffold [11]. Indeed scaffolds crosslinked with 10% of conventional conditions were stable for 28 days in aqueous conditions making them potentially suitable for long-term culture [11]. The cell-biological data presented here show that by employing this

Fig. 12. A) Crystal structure of the integrin α_2 I domain binding to triple-helical GFOGER collagen peptides (taken from [10]). The carboxylic acid side chain on glutamic acid is shown in orange and the metal ion (Mg^{2+}) contained within the binding site of the I domain is shown in pink. This highlights the critical importance of the glutamic acid carboxylic acid side group in the interaction of I domains with cell adhesive GxOGER motifs on collagen. B) Schematic showing potential EDC/NHS activated crosslinking of carboxylic acid side chains on the cell adhesive GxOGER motifs on collagen with adjacent amine groups on lysine side chains. After crosslinking the carboxylic acid side chain is converted into a peptide bond, rendering it unavailable for integrin binding, resulting in lower levels of integrin-mediated cell adhesion. (For interpretation of the references to colour in this figure legend, the reader is referred to the web version of this article.)

same 10% EDC/NHS concentration native-like cell adhesion can be retained. As such this data allows for the first time the fabrication of a truly biologically compatible EDC/NHS stabilised collagen-based material through the rational design of the crosslinking conditions.

5. Conclusions

Optimal, physiologically-relevant cellular interactions are critical for biomaterial function as tissue engineering substrates. Here we show that carbodiimide crosslinking, as frequently used to stabilise biopolymer scaffolds, influences cell adhesion to collagen. Most significantly, both the affinity and the mode of cell interaction are modulated by carbodiimide treatment. Metal-ion-dependent integrin binding is essentially lost and is replaced with metal-ion-independent adhesion upon carbodiimide crosslinking of scaffolds. This observation was consistent across all four of the collagen binding integrins. Recombinant integrin I domains confirmed that this was an integrin I domain mediated effect. The altered cell interactions lead to a decrease in the cellular spreading,

survival and growth on carbodiimide-treated collagen, highlighting the need to preserve cell-binding activity during scaffold crosslinking regimes by retaining the appropriate biomaterials chemistry. Spatial control of collagen crosslinking allowed for controlled cell attachment which has many applications in regenerative medicine and the study of cell-matrix interactions. Consequently, this research is pivotal to the advancement and efficacy of collagen-based scaffolds.

Acknowledgements

Appendix A. Supplementary data

Supplementary data associated with this article can be found, in the online version, at http://dx.doi.org/10.1016/j.actbio.2016.11.059.

References

[1] C.H. Lee, A. Singla, Y. Lee, Biomedical applications of collagen, Int. J. Pharm. 221 (2001) 1–22.

[2] K.E. Kadler, C. Baldock, J. Bella, R.P. Boot-Handford, Collagens at a glance, J. Cell Sci. 120 (2007) 1955–1958.

[3] L. Cen, W. Liu, L. Cui, W. Zhang, Y. Cao, Collagen tissue engineering: development of novel biomaterials and applications, Pediatr. Res. 63 (2008) 492–496.

[4] S. Hamaia, R.W. Farndale, Integrin recognition motifs in the human collagens, Adv. Exp. Med. Biol. 819 (2014) 127–142.

[5] D. Sheppard, The role of integrins in pulmonary fibrosis, Eur. Respir. Rev. 17 (2008) 157–162.

[6] J.D. Humphries, A. Byron, M.J. Humphries, Integrin ligands at a glance, J. Cell Sci. 119 (2006) 3901–3903.

[7] M. Barczyk, S. Carracedo, D. Gullberg, Integrins, Cell Tissue Res. 339 (2010) 269–280.

[8] R.W. Farndale, T. Lisman, D. Bihan, S. Hamaia, C.S. Smerling, N. Pugh, A. Konitsiotis, B. Leitinger, P.G. de Groot, G.E. Jarvis, N. Raynal, Cell-collagen interactions: the use of peptide Toolkits to investigate collagen-receptor interactions, Biochem. Soc. Trans. 36 (2008) 241–250.

[9] P.R. Siljander, S. Hamaia, A.R. Peachey, D.A. Slatter, P.A. Smethurst, W.H. Ouwehand, C.G. Knight, R.W. Farndale, Integrin activation state determines selectivity for novel recognition sites in fibrillar collagens, J. Biol. Chem. 279 (2004) 47763–47772.

[10] J. Emsley, C.G. Knight, R.W. Farndale, M.J. Barnes, R.C. Liddington, Structural basis of collagen recognition by integrin alpha2beta1, Cell 101 (2000) 47–56.

[11] N. Davidenko, C.F. Schuster, D.V. Bax, N. Raynal, R.W. Farndale, S.M. Best, R.E. Cameron, Control of crosslinking for tailoring collagen-based scaffolds stability and mechanics, Acta Biomater. 25 (2015) 131–142.

[12] C.N. Grover, R.E. Cameron, S.M. Best, Investigating the morphological, mechanical and degradation properties of scaffolds comprising collagen, gelatin and elastin for use in soft tissue engineering, J. Mech. Behav. Biomed. Mater. 10 (2012) 62–74.

[13] K.M. Pawelec, A. Husmann, S.M. Best, R.E. Cameron, A design protocol for tailoring ice-templated scaffold structure, J. R. Soc. Interface 11 (2013) 20130958.

[14] K.M. Pawelec, A. Husmann, S.M. Best, R.E. Cameron, Altering crystal growth and annealing in ice-templated scaffolds, J. Mater. Sci. 50 (2015) 7537–7543.

[15] J.C. Ashworth, M. Mehr, P.G. Buxton, S.M. Best, R.E. Cameron, Parameterizing the transport pathways for cell invasion in complex Scaffold architectures, Tissue Eng. Part C Methods 22 (2016) 409–417.

[16] J.C. Ashworth, M. Mehr, P.G. Buxton, S.M. Best, R.E. Cameron, Cell invasion in collagen Scaffold architectures characterized by percolation theory, Adv. Healthc. Mater. 4 (2015) 1317–1321.

[17] C.F. Tiger, F. Fougerousse, G. Grundstrom, T. Velling, D. Gullberg, Alpha11beta1 integrin is a receptor for interstitial collagens involved in cell migration and collagen reorganization on mesenchymal nonmuscle cells, Dev. Biol. 237 (2001) 116–129.

[18] M.J. Humphries, Cell adhesion assays, Mol. Biotechnol. 18 (2001) 57–61.

[19] S.W. Hamaia, N. Pugh, N. Raynal, B. Nemoz, R. Stone, D. Gullberg, D. Bihan, R.W. Farndale, Mapping of potent and specific binding motifs, GLOGEN and GVOGEA, for integrin alpha1beta1 using collagen toolkits II and III, J. Biol. Chem. 287 (2012) 26019–26028.

[20] R.W. Farndale, D.A. Slatter, P.R. Siljander, G.E. Jarvis, Platelet receptor recognition and cross-talk in collagen-induced activation of platelets, J. Thromb. Haemost. 5 (Suppl. 1) (2007) 220–229.

[21] N. Raynal, S.W. Hamaia, P.R. Siljander, B. Maddox, A.R. Peachey, R. Fernandez, L.J. Foley, D.A. Slatter, G.E. Jarvis, R.W. Farndale, Use of synthetic peptides to locate novel integrin alpha2beta1-binding motifs in human collagen III, J. Biol. Chem. 281 (2006) 3821–3831.

[22] S. Perret, J.A. Eble, P.R. Siljander, C. Merle, R.W. Farndale, M. Theisen, F. Ruggiero, Prolyl hydroxylation of collagen type I is required for efficient binding to integrin alpha 1 beta 1 and platelet glycoprotein VI but not to alpha 2 beta 1, J. Biol. Chem. 278 (2003) 29873–29879.

[23] C.G. Knight, L.F. Morton, A.R. Peachey, D.S. Tuckwell, R.W. Farndale, M.J. Barnes, The collagen-binding A-domains of integrins alpha(1)beta(1) and alpha(2)beta(1) recognize the same specific amino acid sequence, GFOGER, in native (triple-helical) collagens, J. Biol. Chem. 275 (2000) 35–40.

[24] G. Lammers, G.S. Tjabringa, J. Schalkwijk, W.F. Daamen, T.H. van Kuppevelt, A molecularly defined array based on native fibrillar collagen for the assessment of skin tissue engineering biomaterials, Biomaterials 30 (2009) 6213–6220.

[25] C.N. Grover, R.W. Farndale, S.M. Best, R.E. Cameron, The interplay between physical and chemical properties of protein films affects their bioactivity, J. Biomed. Mater. Res. A 100 (2012) 2401–2411.

[26] C.N. Grover, J.H. Gwynne, N. Pugh, S. Hamaia, R.W. Farndale, S.M. Best, R.E. Cameron, Crosslinking and composition influence the surface properties, mechanical stiffness and cell reactivity of collagen-based films, Acta Biomater. 8 (2012) 3080–3090.

[27] J.D. Malcor, D. Bax, S.W. Hamaia, N. Davidenko, S.M. Best, R.E. Cameron, R.W. Farndale, D. Bihan, The synthesis and coupling of photoreactive collagen-based peptides to restore integrin reactivity to an inert substrate, chemically-crosslinked collagen, Biomaterials 85 (2016) 65–77.

[28] D. Enea, F. Henson, S. Kew, J. Wardale, A. Getgood, R. Brooks, N. Rushton, Extruded collagen fibres for tissue engineering applications: effect of crosslinking method on mechanical and biological properties, J. Mater. Sci. – Mater. Med. 22 (2011) 1569–1578.

[29] Z. Ahmad, J.H. Shepherd, D.V. Shepherd, S. Ghose, S.J. Kew, R.E. Cameron, S.M. Best, R.A. Brooks, J. Wardale, N. Rushton, Effect of 1-ethyl-3-(3-dimethylaminopropyl) carbodiimide and N-hydroxysuccinimide concentrations on the mechanical and biological characteristics of cross-linked collagen fibres for tendon repair, Regen. Biomater. 2 (2015) 77–85.

[30] M.G. Haugh, C.M. Murphy, R.C. McKiernan, C. Altenbuchner, F.J. O'Brien, Crosslinking and mechanical properties significantly influence cell attachment, proliferation, and migration within collagen glycosaminoglycan scaffolds, Tissue Eng. Part A 17 (2011) 1201–1208.

[31] L. Salvatore, M. Madaghiele, C. Parisi, F. Gatti, A. Sannino, Crosslinking of micropatterned collagen-based nerve guides to modulate the expected half-life, J. Biomed. Mater. Res. A 102 (2014) 4406–4414.

[32] K. Nam, T. Kimura, S. Funamoto, A. Kishida, Preparation of a collagen/polymer hybrid gel for tissue membranes. Part II: in vitro and in vivo biological properties of the collagen gels, Acta Biomater. 6 (2010) 409–417.

[33] L. Buttafoco, P. Engbers-Buijtenhuijs, A.A. Poot, P.J. Dijkstra, W.F. Daamen, T.H. van Kuppevelt, I. Vermes, J. Feijen, First steps towards tissue engineering of small-diameter blood vessels: preparation of flat scaffolds of collagen and elastin by means of freeze drying, J. Biomed. Mater. Res. B Appl. Biomater. 77 (2006) 357–368.

[34] M.J. Wissink, M.J. van Luyn, R. Beernink, F. Dijk, A.A. Poot, G.H. Engbers, T. Beugeling, W.G. van Aken, J. Feijen, Endothelial cell seeding on crosslinked collagen: effects of crosslinking on endothelial cell proliferation and functional parameters, Thromb. Haemost. 84 (2000) 325–331.

[35] G.P. Huang, S. Shanmugasundaram, P. Masih, D. Pandya, S. Amara, G. Collins, T. L. Arinzeh, An investigation of common crosslinking agents on the stability of electrospun collagen scaffolds, J. Biomed. Mater. Res. A 103 (2015) 762–771.

[36] W.H. Tiong, G. Damodaran, H. Naik, J.L. Kelly, A. Pandit, Enhancing amine terminals in an amine-deprived collagen matrix, Langmuir 24 (2008) 11752–11761.

[37] J. Li, N. Ren, J. Qiu, H. Jiang, H. Zhao, G. Wang, R.I. Boughton, Y. Wang, H. Liu, Carbodiimide crosslinked collagen from porcine dermal matrix for high-strength tissue engineering scaffold, Int. J. Biol. Macromol. 61 (2013) 69–74.

[38] R. Pankov, K.M. Yamada, Fibronectin at a glance, J. Cell Sci. 115 (2002) 3861–3863.

[39] M.A. Horton, The alpha v beta 3 integrin "vitronectin receptor", Int. J. Biochem. Cell Biol. 29 (1997) 721–725.

[40] M.C. Erat, B. Sladek, I.D. Campbell, I. Vakonakis, Structural analysis of collagen type I interactions with human fibronectin reveals a cooperative binding mode, J. Biol. Chem. 288 (2013) 17441–17450.

[41] K. Sano, K. Asanuma-Date, F. Arisaka, S. Hattori, H. Ogawa, Changes in glycosylation of vitronectin modulate multimerization and collagen binding during liver regeneration, Glycobiology 17 (2007) 784–794.

[42] G.J. Her, H.C. Wu, M.H. Chen, M.Y. Chen, S.C. Chang, T.W. Wang, Control of three-dimensional substrate stiffness to manipulate mesenchymal stem cell fate toward neuronal or glial lineages, Acta Biomater. 9 (2013) 5170–5180.

[43] N. Davidenko, C.F. Schuster, D.V. Bax, R.W. Farndale, S. Hamaia, S.M. Best, R.E. Cameron, Evaluation of cell binding to collagen and gelatin: a study of the

effect of 2D and 3D architecture and surface chemistry, J. Mater. Sci. – Mater. Med. 27 (2016) 148.

[44] J. El-Ali, P.K. Sorger, K.F. Jensen, Cells on chips, Nature 442 (2006) 403–411.

[45] A. Ohl, K. Schroder, Plasma-induced chemical micropatterning for cell culturing applications: a brief review, Surf. Coat Tech. 119 (1999) 820–830.

[46] W. Tan, T.A. Desai, Microfluidic patterning of cells in extracellular matrix biopolymers: effects of channel size, cell type, and matrix composition on pattern integrity, Tissue Eng. 9 (2003) 255–267.

[47] Z. Nie, E. Kumacheva, Patterning surfaces with functional polymers, Nat. Mater. 7 (2008) 277–290.